Available online at www.sciencedirect.com
SCIENCE DIRECT®
Global and Planetary Change 38 (2003) 121–135
GLOBAL AND PLANETARY CHANGE
www.elsevier.com/locate/gloplacha

The CHAmeleon Surface Model: description and use with the PILPS phase 2(e) forcing data

A.J. Pitman[a,*], Y. Xia[a], M. Leplastrier[a], A. Henderson-Sellers[b]

[a] *Department of Physical Geography, Macquarie University, North Ryde, NSW 2109, Sydney, Australia*
[b] *Environment Division, Australian Nuclear Science and Technology Organization, Sydney, Australia*

Received 19 November 2001; received in revised form 16 February 2002; accepted 24 March 2002

Abstract

The CHAmeleon Surface Model (CHASM) is used with the Project for the Intercomparison of Land-surface Parameterization Schemes (PILPS) Phase 2(e) experimental design. The model, with five levels of surface energy complexity, is shown to simulate the observed runoff for two sub-basins within the PILPS 2e domain with some degree of skill. This skill is shown to be largely insensitive to the complexity of the surface energy balance (SEB) parameterization, provided that a spatially and temporally constant surface resistance is used. While all bar the least complex mode of CHASM works reasonably (within 5% of the observed runoff at Ovre Abiskojokk and within 15–20% at Ovre Lansjarv), there are weaknesses in the simulations, particularly at a seasonal time scale. It is shown that these deficiencies are unlikely be caused by the complexity of the surface energy balance formulation. At the scale of the PILPS 2(e) domain, it is shown that the addition of a constant surface resistance into the simplest mode of CHASM has a large impact on runoff by reducing the latent heat flux. It is shown that adding further complexity by including explicit interception and explicit bare soil evaporation has little effect on runoff or the latent heat flux, but the addition of a spatially and temporally variable surface resistance leads to an increase in the spatial variability of runoff across the domain. The differences between the modes of CHASM are then compared against the range of simulations of other models in PILPS Phase 2(e). The difference between the modes of CHASM (excluding the simplest mode, which omits the surface resistance term) is approximately 10–15% of the range in results from the other PILPS schemes. This is argued to be too small to explain the differences found in the results from PILPS Phase 2(e). Given that differences cannot be explained by variations in the SEB complexity, they are most likely to be caused by differences in the hydrology formulation (including snowmelt and snowmelt infiltration).
© 2003 Elsevier Science B.V. All rights reserved.

Keywords: surface energy balance; land surface model; Chameleon land surface model

1. Introduction

The parameterization of land surface processes in climate models affects the simulation of climate (Sato et al., 1989; Verseghy et al., 1993; Crossley et al., 2000; Desborough et al., 2001). The impact of land surface processes occurs largely via a change in the partitioning of available energy between sensible and latent heat, and/or through a change in the partitioning of available water through evaporation and runoff. Attempts to identify the relationship between the way land surface processes are represented, and the way a land surface

* Corresponding author. Tel.: +61-2-9850-8425; fax: +61-2-9850-8420.
E-mail address: apitman@penman.es.mq.edu.au (A.J. Pitman).

0921-8181/03/$ - see front matter © 2003 Elsevier Science B.V. All rights reserved.
doi:10.1016/S0921-8181(03)00015-8

model (LSM) performs has therefore tended to focus on the parameterization of the hydrological and the surface energy balance (SEB) components.

The role of the hydrological component of LSMs has been the subject of considerable attention. Crossley et al. (2000) and Gedney et al. (2000) analyzed the results from four climate models, each coupled to two LSMs and found that surface processes affected the sensitivity of surface temperature and the surface hydrological cycle to increases in CO_2. Gedney et al. (2000) showed that this sensitivity could be attributed to the way the hydrological processes (especially runoff) were parameterized in the models. The recognition of the significance of hydrological processes has led to an increased focus on these processes in LSMs (Wood et al., 1992; Koster et al., 2000; Ducharne et al., 2000).

Traditionally, most effort in LSMs has been paid to the parameterization of the SEB (Sellers et al., 1997). Most LSMs have developed from the micrometeorological approach of Deardorff (1978) and have placed most emphasis on an explicit representation of diurnal scale processes and on how vegetation influences land–atmosphere interactions (see Desborough, 1999). Thus, many recent LSMs have quite complex vertical representations of above ground processes (Sellers et al., 1986, 1996; Noilhan and Planton, 1989; Dickinson et al., 1993; Verseghy et al., 1993; Bonan, 1995; Desborough and Pitman, 1998). The level of complexity required to model the SEB is debatable, given that the recognition of the significant role of the surface hydrology and the realization that the lack of horizontal complexity is a significant omission in LSMs.

In order to examine the role of the SEB, Desborough (1999) developed the CHAmeleon Surface Model (CHASM). CHASM can operate in a variety of modes which attempts to replicate the range of SEB complexity used in those models within the Project for Intercomparison of Land-surface Parameterization Schemes (PILPS, Henderson-Sellers et al., 1995). The range of SEB parameterizations included within CHASM varies from a simple Manabe-type bucket model to more complex mosaic type models (i.e. Deardorff, 1978) with separate surface energy balances for each mosaic tile (e.g. Koster and Suarez, 1992) and explicit treatment of transpiration, canopy interception and bare ground evaporation. A description of CHASM, along with details of how the model attempts to replicate this range in SEB complexity, is presented in Section 2. The purpose of CHASM is to determine what fraction of the differences in the behaviour of LSMs, found in PILPS-type experiments, can be explained solely in terms of SEB complexity. If little variability in results is found by varying the SEB complexity, then it is likely that differences in results obtained by other LSMs are due to other factors. However, if considerable differences are obtained through varying SEB complexity, then these provide guidance in trying to explain the range of results obtained by PILPS (Chen et al., 1997; Pitman et al., 1999; Schlosser et al., 2000). Thus, following details of methodology (Section 2) and an evaluation of the model's performance in PILPS Phase 2(e), CHASM is used to determine the differences in the simulation of runoff and evaporation for the PILPS 2(e) experiments that result from variations in SEB complexity (Section 4). Section 5 discusses the results and concludes.

2. The CHAmeleon Surface Model (CHASM)

In PILPS and in other intercomparison exercises (Polcher et al., 1996; Dirmeyer et al., 1999), various LSMs are compared and assessments are made regarding those differences caused by parameterization or parameter choices. The choice of effective parameter values is known to bias the results from these intercomparison exercises since the appropriate value for a particular parameter is model dependent (Chen et al., 1997; Desborough, 1999). Thus, a more controlled modelling environment is needed to compare differences in simulations caused by differences in parameterizations: an environment where the effects of inter-model parameter variations can be isolated and removed.

With this in mind, the chameleon land surface model (CHASM) was designed (Desborough, 1999). CHASM's design focuses on exploring the impact of SEB complexity on model behaviour rather than addressing every parameterization difference between every model in PILPS-type experiments. The design was influenced by previous work by Koster and Suarez (1994), where differences between a simple LSM (based on the Manabe, 1969 bucket) and a more

complex scheme (based on the Deardorff, 1978 model) were examined. They found that removing the more complex scheme's canopy interception parameterization resulted in substantial decreases in simulated evaporation and precipitation.

CHASM can run with a variety of SEB configurations (or modes, see Table 1) which are discussed in detail later. Each mode is combined with a common soil moisture, snow and soil temperature model. These are briefly discussed next, followed by details of the SEB configurations.

CHASM has proven to be a useful tool in explaining some of the large simulation differences obtained by PILPS (e.g. Desborough, 1999), in identifying the role of the SEB in influencing climate (Desborough et al., 2001) and in identifying the role of the SEB in affecting the sensitivity of climate to doubling atmospheric carbon dioxide (Pitman and McAvaney, 2002). The maintenance of a common modelling environment, as just the SEB changes, ensures that parameters retain the same effective value. This allows the modeller to explore the effect of increasing the complexity of the SEB configuration by sequentially adding explicit parameterizations.

2.1. Basic model parameterization

To resolve the SEB, CHASM combines similar elements throughout a grid square to form tiles (a "grouped mosaic approach", e.g. Koster and Suarez, 1992). Each tile is further divided into aerial cover fractions of vegetation, snow and ground. Snow cover fractions for ground and foliage surfaces are calculated as functions of the snowpack depth and density and the vegetation roughness length, following methods used in earlier LSMs (Cogley et al., 1990; Desborough and Pitman, 1998). The vegetation fraction is further divided into wet and dry fractions if the surface configuration mode allows for canopy interception. Each tile has a prognostic bulk temperature (T_1) for the storage of energy and a diagnostic skin temperature (T_0) for the calculation of surface energy fluxes (Fig. 1). There are individual parameters for shortwave albedo and roughness length for each type of cover (e.g. snow, bare ground and vegetation). The overall surface albedo and roughness length is calculated from an area-weighted approach across the snow, vegetation and bare ground fractions. CHASM also includes seasonality parameters for leaf area index and vegetation fraction.

Soil temperature is simulated to a depth of 4 m with the cross section divided into layers: 0.1–0.4, 0.4–1.0, 1–2 and 2–4 m (Fig. 1). Energy transfers within the soil are represented using a finite difference method with constant values for volumetric heat capacity and thermal conductivity and a zero-flux boundary condition at the base of the profile. CHASM utilises evaporable moisture rather than volumetric soil moisture content to avoid the inclusion of a thermal conductivity reduction for very dry soils.

CHASM's hydrology follows Manabe (1969) in that the root zone is treated as a bucket with finite water holding capacity and beyond this capacity runoff occurs. Runoff also occurs if the fraction of snow cover on the ground exceeds 95% and rainfall occurs. In neither case is runoff re-distributed. Apart from moisture in the root zone, water can also be stored as snow; or depending on the mode, stored on the canopy following interception of precipitation, or on the surface for bare ground evaporation. While the use of a simple hydrology model may seem outdated,

Table 1
Summary of the differences between the CHASM modes used in this paper, indicating which of them includes explicit parameterizations for canopy interception, bare ground evaporation, canopy resistance and horizontal temperature differentiation

CHASM mode	Stability correction	Surface resistance	canopy interception	bare ground evaporation	canopy resistance	temperature differentiation
SLAM	✓	✓	✓	✓	✓	✓
RSGI	✓	✓	✓	✓	–	–
RSI	✓	✓	✓	–	–	–
RS	✓	✓	–	–	–	–
EB	–	–	–	–	–	–

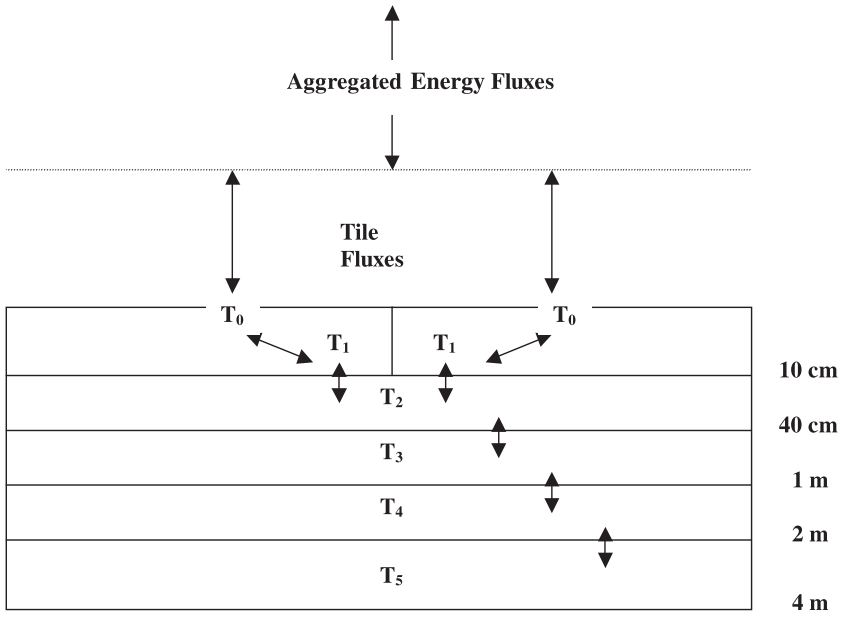

Fig. 1. Schematic representation of the energy parameterization of CHASM's most complex mode, SLAM. The above-ground energy fluxes represent radiation, sensible heat and latent heat fluxes. $T_2 - T_5$ represent sub-surface temperatures to a depth of 4 m. T_1 is a bulk soil temperature and T_0 is a skin temperature. Simpler modes use a single tile for T_0 and T_1.

Robock et al. (1995) have shown it to work well in mid-latitude regions and the use of this hydrology model has not been associated with poor performance in earlier PILPS experiments.

The snow scheme assumes that the precipitation falls as snow if the near surface air temperature is below 0 °C. The snowpack is represented by one composite layer (see Slater et al., 2001). The albedo is modified as a function of snow age and the fractional cover of snow is calculated as a function of the snow depth and density (Kojima, 1967) combined with the roughness length of vegetation (Desborough and Pitman, 1998). Snow density in CHASM increases over time as a result of mechanical compaction from overlying snow and decreases when new snow falls. The thermal conductivity is represented as a function of snow density (Desborough and Pitman, 1998). The available energy to melt snow is computed as residual of the SEB and/or soil heat energy. Any meltwater is added to the soil moisture store, or becomes runoff.

Each tile, depending on the mode, can have up to four evaporation sources: canopy evaporation, transpiration, bare ground evaporation and snow sublimation. Again, depending on the mode, resistances may

Fig. 2. Illustration of the structure of CHASM for each mode discussed in the text. (a) The simplest mode EB includes two principal evaporation sources, evaporation from the root zone (E_{tr}) and the snow pack (E_n). An additional flux required in the two-tiled approach is E'_{tr}, which is from the snow-free portion of Tile B and is calculated identically to E_{tr}. Two moisture storage terms represent the root zone (W_r) and the snow pack (W_n). The aerodynamic resistance (r_a) is calculated without an atmospheric stability constant; (b) mode RS where r_a is calculated with an atmospheric stability constant and r_s is added to the resistance pathway of E_{tr} and E'_{tr}; (c) mode RSI adds canopy interception storage (W_c) and the accompanying flux (E_c); (d) mode RSGI adds a bare ground parameterization, an extra moisture storage term (W_g) and an extra evaporative source (E_g); (e) mode SLAM divides the surface into two tiles and the temporally invariant surface resistance r_s, used in simpler modes, is replaced by a variable canopy resistance r_c, which is applied to the evaporation pathway, E_{tr}. Other terms include ρ_a (air density), A^t (the size of tile A), q (specific humidity of the surface, q^* and the air, q_a), β is a wetness factor and a_n, a_{wet}, a_{dry} are the fractions of snow, wet canopy and dry canopy, respectively.

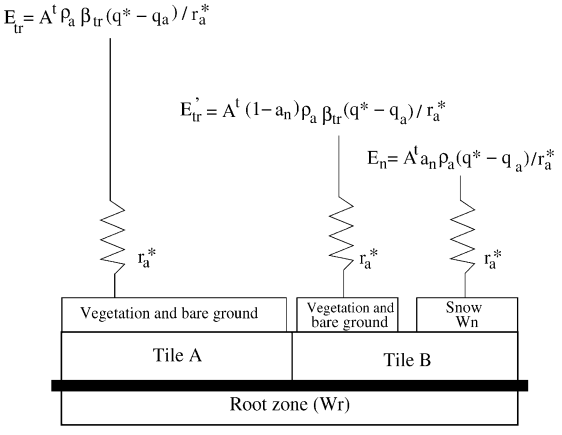

(a) EB

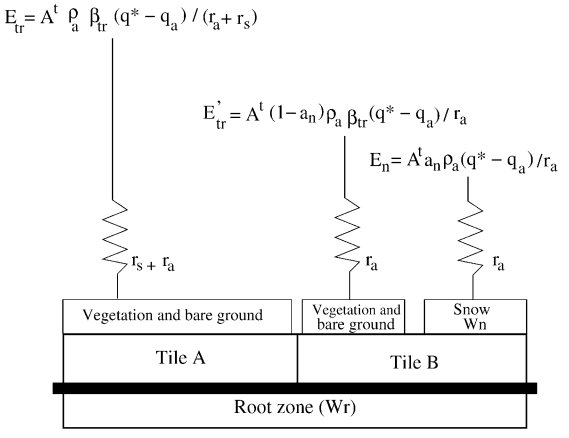

(b) RS

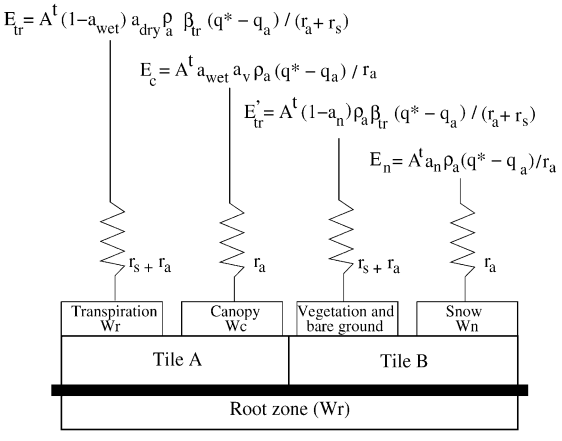

(c) RSI

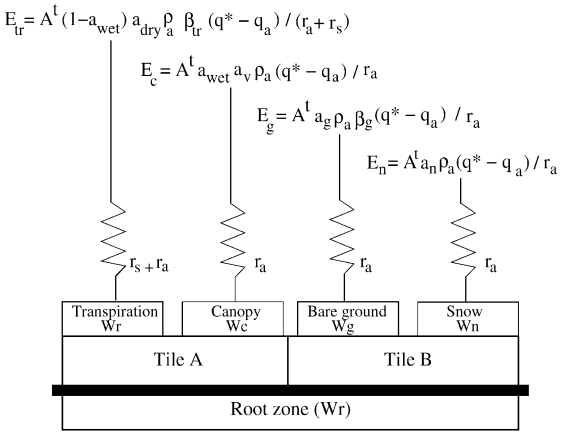

(d) RSGI

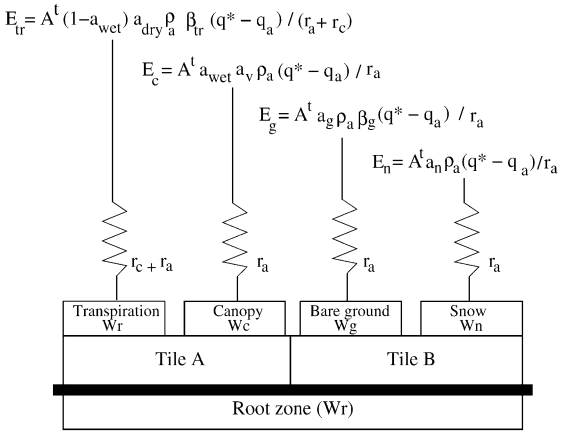

(e) SLAM

be applied to reduce evaporation and transpiration rates. As these resistances and the different ways in which they are applied are a key part of the differences between modes, they will be described in detail in the next section.

Due to the prescription of 100% vegetation cover at Ovre Lansjarv in the PILPS 2e experimental design, the one-tile approach used in most modes of CHASM did not perform well in the presence of snow. This is not a problem of modelling snow since the model performed well using one tile for the alternative catchment (Ovre Abiskojokk). To deal with the problem of 100% vegetation cover and snow cover, which CHASM was not designed to cope with (since this would not occur within a climate model), CHASM was extended to include a separate tile for snow. This had little effect on results from Ovre Abiskojokk, or results in the snow-free period at Ovre Lansjarv, but substantially improved the model performance in winter at Ovre Lansjarv.

This is likely to be related to the model structure of CHASM rather than anything generic about the way snow should be modelled in LSMs and is therefore not discussed in further detail here.

2.2. CHASM's modes

Table 1 lists the different modes of CHASM used in this study in increasing order of complexity. The features that differentiate the modes are also listed and described in detail below.

EB is the simplest mode of CHASM. In its usual implementation, the surface is constructed from one tile so the fraction of the surface occupied by the tile, A^t, equals one. However, in this paper, two tiles are used with snow and bare soil processes are dealt with separately. Since the prescribed bare soil fraction is small (and zero at Ovre Lansjarv), in effect, the second tile is restricted to snow and the non-snow-covered fraction $(1 - A_n)$ is being treated identically to tile A (see Fig. 2a). The aerodynamic resistance to turbulent transport for heat and moisture (r_a) is calculated without an atmospheric stability constant (and is thus denoted r_a^*) to parallel the model used by Koster and Milly (1997). Moisture available for evaporation is only stored in the root zone (W_r) and on the surface as snow (W_n) so there are only two evaporation sources, evaporation from the snow (E_n) and evaporation from the root zone (E_{tr}) to which r_a is applied (Fig. 2a). a_n represents the fraction of the surface covered by snow. E_{tr} is reduced below the potential rate by an additional moisture availability resistance (β_{tr}). The calculation of E_{tr} and E_n also involves the density of air (ρ_a), the surface saturated specific humidity (q_a^*) (calculated as a function of T_0) and specific humidity of the air (q_a).

Mode RS is the same as EB but with a temporally invariant surface resistance (r_s) added to the resistance pathway of snow-free evaporation. Also r_a is calculated with an atmospheric stability correction (see Fig. 2b).

Mode RSI builds onto the RS mode by adding an explicit parameterization for canopy interception of precipitation (Fig. 2c). There are, therefore, three evaporation sources with the inclusion of evaporation of intercepted water (E_c) following the addition of storage of water within the canopy (W_c). The canopy is divided into fractions of wet (a_{wet}) and dry (a_{dry}) areas which are dependent on the amount of precipitation and evaporation rates.

Mode RSGI adds bare ground evaporation to the RSI mode. Moisture can be stored at the surface for evaporation up to a maximum of 40 kg/m^2. Bare ground evaporation is affected by moisture availability where a resistance, β_g, is included in the evaporation pathway. β_g reduces bare ground evaporation linearly to zero as moisture availability reduces to zero. The RSGI mode is illustrated in Fig. 2d and includes four evaporation fluxes (E_{tr}, E_c, E_n and E_g) and their corresponding moisture storage terms (W_r, W_c, W_n and W_g).

In the standard implementation of CHASM, the most complex mode (SLAM) is the same as RSGI but the land atmosphere interface is divided into two tiles with one representing a combination of bare ground and exposed snow, and the other reserved for vegetation and the surface resistance is temporally and spatially variable. The rationale for tiling the land surface is discussed by Koster and Suarez (1992), but basically, it is an attempt to include surface heterogeneity in the LSM. The tiles are not necessarily the same size as they are area weighted depending on the individual fractions of the land surface type. A separate SEB is calculated for each tile which allows for temperature variations across the land atmosphere interface, a feature not usually present in the less complex modes. However, given

the use of two tiles in all modes used in PILPS 2(e), the only change between RSGI and SLAM is the time step calculation of a variable canopy resistance, r_c, which replaces the constant surface resistance, r_s, in the calculation of E_{tr} used in RS, RSI and RSGI modes.

3. Methodology

Five CHASM modes are used to perform 20-year (1979–1998) simulations for the Torne/Kalix River system in northern Scandinavia. The last 10 years (1989–1998) of each simulation are used to analyse and compare the performance of the each mode of the model. The PILPS 2(e) experiment design was followed. Atmospheric forcing data were used with a 1-h interval and forcing data from 1979 to 1988 were used for model 'spin up'. The period of 1989–1998 was selected for intercomparison and analysis of CHASM's modes. Full details of the methodology and available observations are available in Bowling et al. (in press).

In using CHASM, the most complex mode, SLAM, is assumed to be the best on the basis that a higher proportion of the parameterizations used in the SEB calculations are explicit and physically based. The other modes, where the surface resistance term is fixed (RS, RSI and RSGI) are therefore calibrated (varying only surface resistance) to match the long-term (20 years) average simulation of evaporation by SLAM averaged over the entire PILPS 2(e) domain. While modes RS, RSI, RSGI and SLAM simulate virtually identical total evaporation over the total length of simulation, the modes can vary substantially on the annual or seasonal time scale. This calibration is fundamental to our experimental design. The parameter-calibrated, surface resistance cannot be measured directly and hence we do not know what the "correct" value should be. Further, the "correct" value is scheme dependent (Chen et al., 1997; Desborough, 1999) and varies as the representation of some processes are included in a model (e.g. interception). We use surface resistance as a parameter to adjust average evaporation so that the long-term average evaporation (over 20 years) is the same between modes (see Desborough, 1999 for more details). Analysis of the impact of changes in the SEB then concentrates on time scales well below decadal and/or spatial scales well below the entire domain; since at these timescales, the calibration of surface resistance does not imply that runoff, evaporation, etc. should necessarily be similar if the SEB is affecting model results.

Table 2
Observed and simulated annual runoff (mm), averaged over 10 years (1989–1998) at the Ovre Abiskojokk and Ovre Lansjarv basin

Basin	Observed	SLAM	RSGI	RSI	RS	EB
Ovre Abiskojokk	838.6	872.9	863.6	858.4	855.8	672.8
Ovre Lansjarv	349.6	433.0	412.6	414.3	405.4	218.5

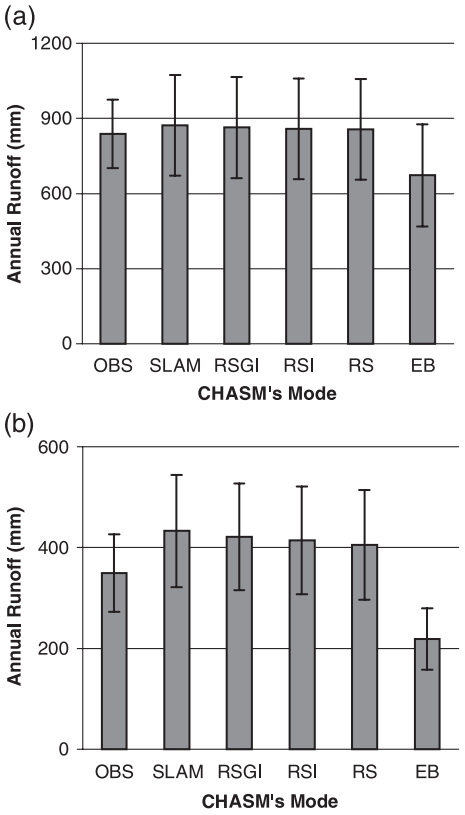

Fig. 3. Annually averaged simulation of runoff for each mode of CHASM and observed for (a) Ovre Abiskojokk and (b) Ovre Lansjarv (mm). These are averaged over the two catchments and over the second 10-year period (1989–1998) of the simulations. The standard deviations (of the interannual variability) are shown as bars.

4. Validation of simulated runoff with observed data

4.1. Annual and seasonal runoff

The very simple parameterization of runoff included in all modes of CHASM (a Manabe, 1969 type formulation) would suggest that the model would not be able to simulate catchment scale runoff particularly well. The observed and simulated annual runoff (averaged over the second 10 years) at the two sub-basins are given in Table 2 and Fig. 3. The results show that the four more complex CHASM modes (SLAM, RSGI, RSI RS) give similar results to each other and to observed runoff. All four modes are within 5% of the observed runoff at Ovre Abiskojokk and their standard deviations are similar (although larger) than the observed (Fig. 3). Mode EB is relatively poor, underestimating the observed runoff by 20%. At Ovre Lansjarv, the simulations are not as good with SLAM simulating runoff of 20% too high, gradually reducing to a 15% overestimate for mode RS (see Table 2 and Fig. 3). Mode EB underestimates annual runoff by 38%. Again, the simulations of the standard deviations are reasonable, although slightly larger than the observed (Fig. 3).

Fig. 4 shows the seasonal pattern of simulated and observed runoff for the two basins. At Ovre Abiskojokk (Fig. 4a), the four more complex modes perform almost identically. All simulate too high a runoff peak occurring about 10 days too early. They also all simulate too rapid a decline in the hydrograph such that negligible runoff is simulated by the end of July, in contrast with the observed which is still about 5 mm day^{-1}. EB simulates a much lower runoff peak, more than a month early, and then simulates negligible runoff from the end of June. This lack of runoff is not related to the hydrological formulation which is identical in all five modes, rather it is the result of excessive evaporation due to the lack of a surface resistance.

A similar result is obtained for Ovre Lansjarv (Fig. 4b), where mode EB simulates too rapid a decline in runoff, and then zero runoff for most of the rest of the year. The other modes also simulate a slightly high and slightly early runoff peak, but then simulate runoff very well through the rest of the year. Again, this improved performance must be the result of

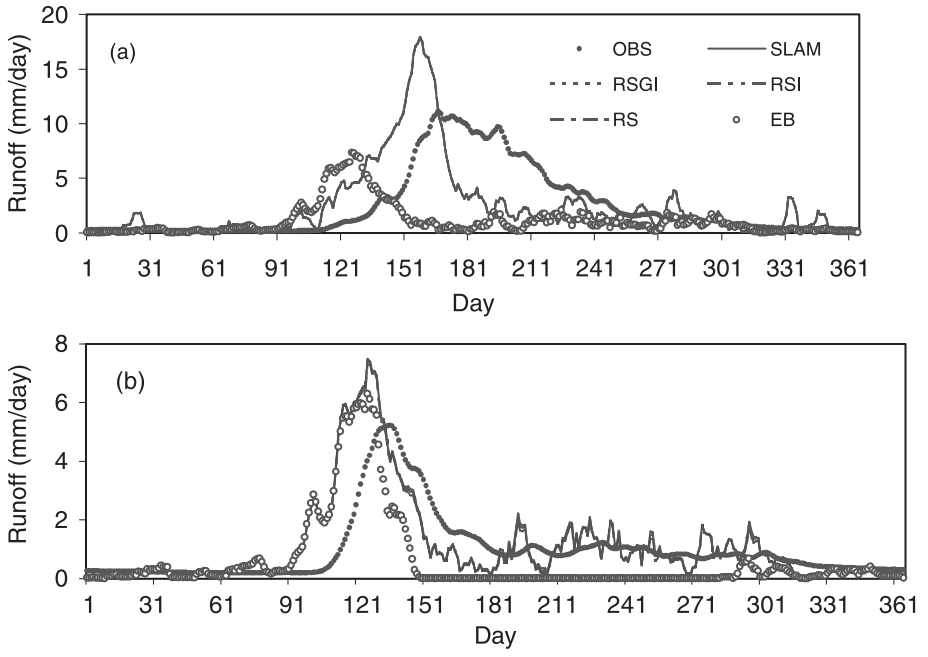

Fig. 4. Seasonal simulation of runoff for each mode of CHASM and observed for (a) Ovre Abiskojokk and (b) Ovre Lansjarv (mm day^{-1}). Note that the results for SLAM, RSGI, RSI and RS are indistinguishable.

simulating evaporation more realistically in the more complex modes, since it is only in the representation of the evaporation pathways that these modes differ.

Overall, therefore, CHASM's simulation of runoff peaks too early resulting in a premature drop in streamflow compared to the observed. There is no substantial difference in the annual or daily runoff between the four more complex modes and all simulate a reasonable seasonal and annual runoff. In particular, all four more complex modes of CHASM simulate runoff well at Ovre Lansjarv from around June and at Ovre Abiskojokk from the end of August. Mode EB performs poorly at both basins not because of the hydrological parameterization, which is the same across all five modes, but because of the simulation of excessive evaporation. The apparently good simulation of runoff by modes RS, RSI and RSGI needs to be considered in terms of the calibration of these modes, using the surface resistance to SLAM over the first 10-years of the data. Without this calibration, the performance of these modes would strongly depend on the choice of the surface resistance value and the suitability of this choice to the particular mode.

The limitations in the simulation of runoff by all more complex modes may relate to problems in the simulation of either runoff or evaporation. Given the lack of sensitivity to the simulation of evaporation across the range of complexity represented by RS to

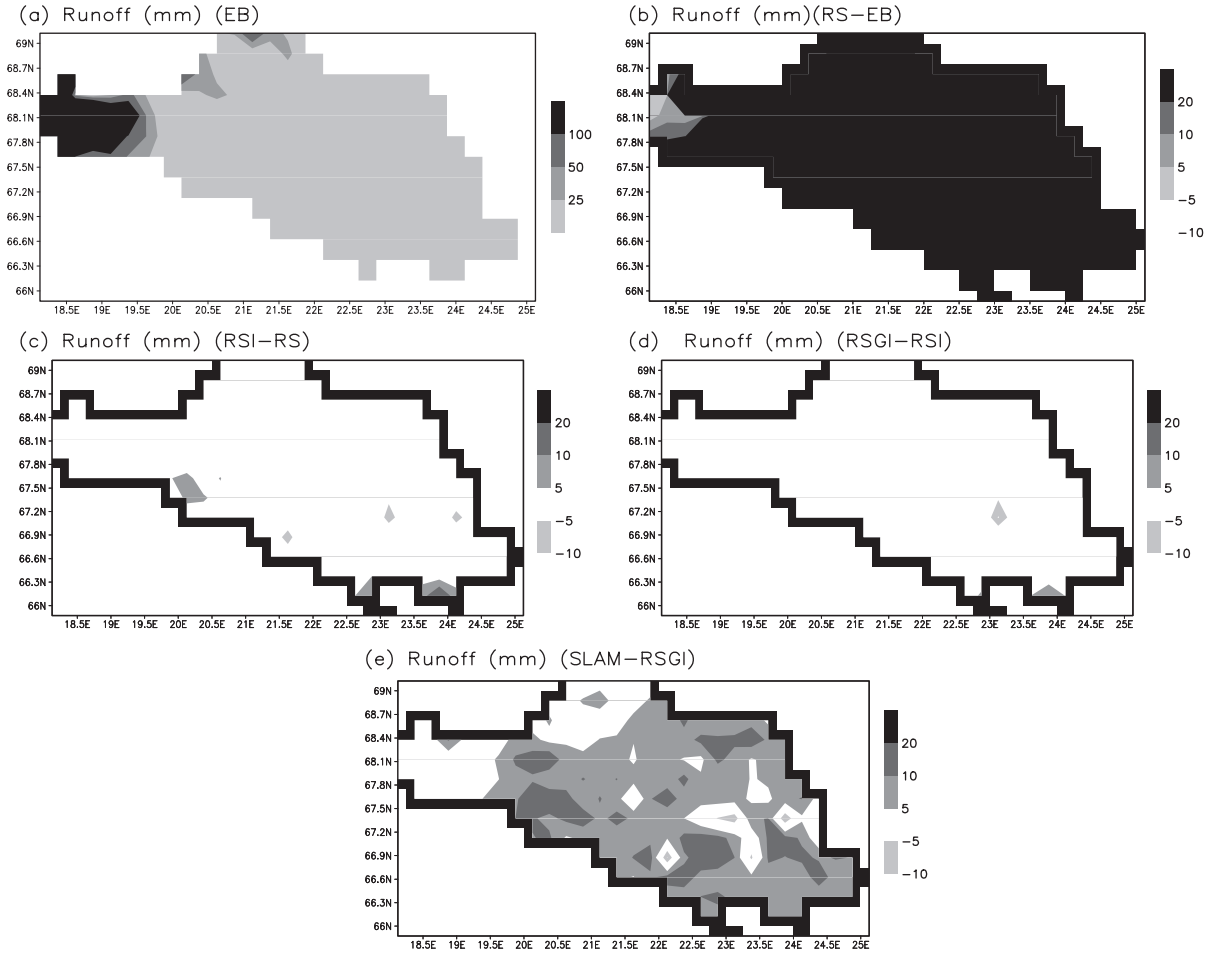

Fig. 5. Simulation of runoff over the PILPS 2(e) domain for June (averaged over the last 3 years of simulation). Mode EB is shown as actual runoff (mm) while the more complex modes are shown as percentage difference from the next simplest mode.

SLAM, it is most likely that these problems are not related to the SEB, rather they are caused by limitations in the hydrological formulation or the lack of river routing. We explored the sensitivity of the results to the water holding capacity and large variations in this parameter (doubling and halving from the specified values) made little difference to the annually averaged sensible or latent heat fluxes (less than 1 W m^{-2}).

4.2. Sensitivity of basin-scale runoff to SEB complexity

While the spatially integrated results from the four most complex modes of CHASM show almost identical behaviour, this can mask significant spatial differences. Fig. 4 shows the simulation of runoff for each mode of CHASM over the entire PILPS 2e domain. We have selected results from June, averaged over the last 3 years of model simulation, to show the impact of changes in the SEB complexity because June is a transition season in this region from snowmelt-induced runoff to precipitation-induced runoff and is therefore a key period to focus upon. The simulation for EB is shown as actual runoff, while the other modes' results are shown as percentage change from the previous (simpler) mode. This permits the impact of specific additions into the SEB formulation to be identified.

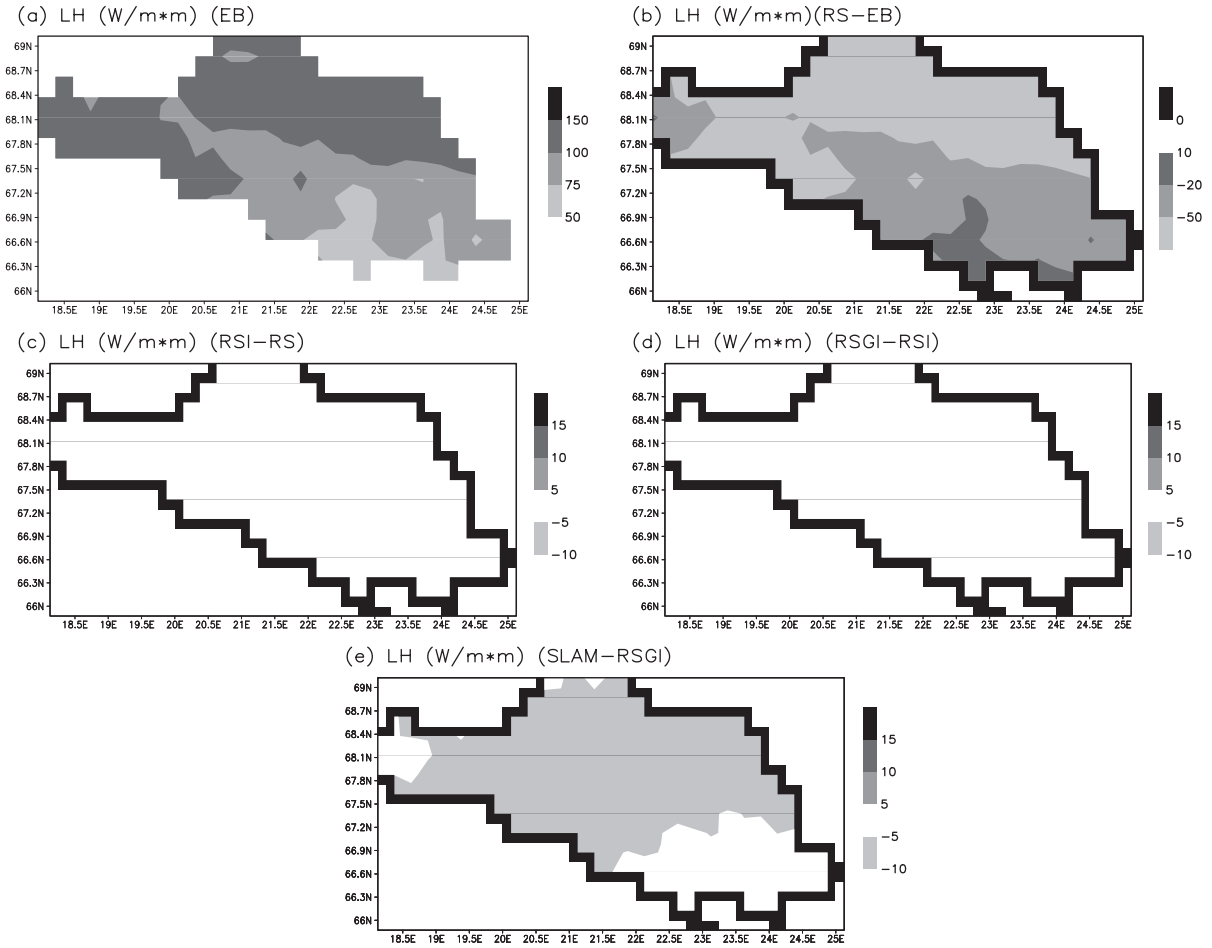

Fig. 6. Simulation of latent heat flux (W m^{-2}) over the PILPS 2(e) domain for June (averaged over the last 3 years of simulation). All modes are as the actual fluxes, differenced from the immediately simpler mode.

Fig. 5b shows the impact of adding a constant surface resistance into mode EB (Fig. 5a). The impact on runoff is very substantial with large increases in runoff over virtually the entire domain. This increase in runoff is caused by the reduction in the latent heat flux (Fig. 6), which is reduced following the imposition of a surface resistance by more than 20 W m^{-2} over almost the entire domain. The addition of an explicit parameterization of interception (Fig. 5c) and explicit bare soil evaporation (Fig. 5d) has little effect on runoff or the latent heat flux (Fig. 6c and d). However, the addition of a spatially and temporally variable surface resistance in the change between RSGI and SLAM does lead to an increase in the variability of runoff across the domain (Fig. 5e) and a small reduction ($\sim 5-10$ W m^{-2}) in the latent heat flux, although the nett change in runoff (Fig. 5e) is very small (5–10%). These changes in runoff, driven directly by changes in the SEB formulation, lead to changes in temperature (Fig. 7). The addition of the resistance term to EB, which reduces the latent heat flux, causes warming across the domain of 0.1 K in the southeastern half and warming of more than 1 K in the northern and western part of the domain. Further increases in SEB complexity have little effect, although the addition of spatially and temporally variable surface resistance does lead to local warming (Fig. 7e) in the northern part of the domain.

Overall, therefore, the major impact on runoff occurs in the initial step of adding a spatially and temporally fixed surface resistance onto mode EB. This reduces evaporation and allows a major increase

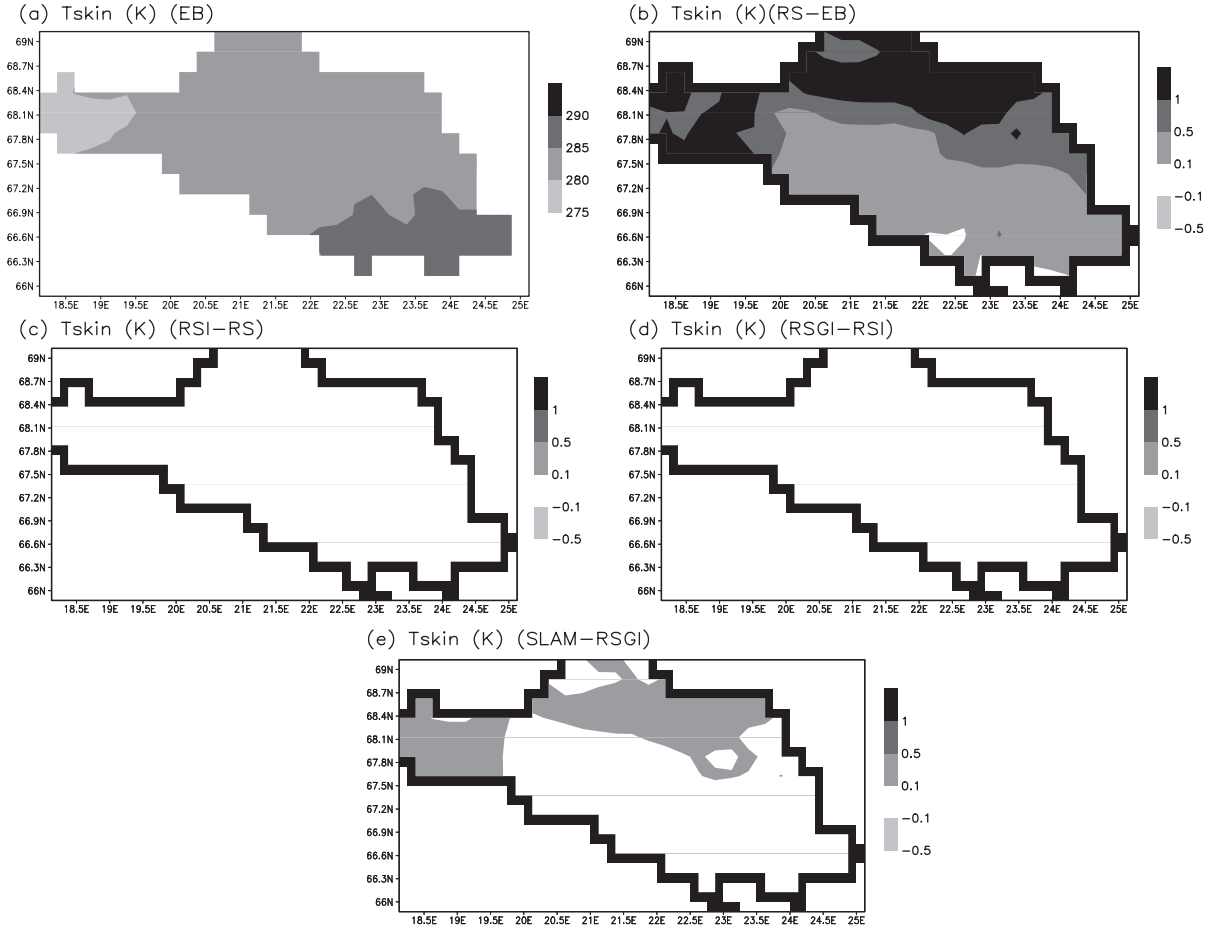

Fig. 7. Same as Fig. 6, but for skin temperature (K).

in runoff and probably an improved simulation (based on the results shown in Figs. 3 and 4). The addition of further complexity has little effect until the surface resistance is allowed to vary spatially and temporally (SLAM). The impact of spatially and temporally varying resistance is mainly ± 5%, but is locally larger (Fig. 5) and may be large enough to support the need for this more complex level of SEB parameterization if the pattern, as distinct from the amount, of runoff is required.

5. Impact of SEB complexity on PILPS 2e results

The results from CHASM show relatively little sensitivity to the complexity of the SEB in the simulation of the seasonal or spatial pattern of runoff, latent heat flux or temperature once a spatially and temporally fixed surface resistance is included. However, the definition of "relatively little sensitivity" is rather subjective. One way of deciding whether the differences in the results from CHASM are, or are not, important is to compare the results from all five modes with those results from other models involved in PILPS Phase 2(e).

Fig. 8a shows the variation in the partitioning of available water between evaporation and runoff. This partitioning ranges across virtually the entire possible scale from one model, which partitions 22% of precipitation into runoff up to another model, which partitions 68% into runoff. EB is the model with the second lowest runoff of all the PILPS 2(e) models and is therefore towards the extreme of the range in Fig. 8a, partitioning 36% of precipitation into runoff. The other four modes of CHASM are at the opposite end of the range and partition 64.6–68.1% of precipitation into runoff (a 3.5% variation). All four more complex modes are within the range of simulations obtained from the other modes. The sensitivity occurring as a result of the SEB complexity change in CHASM can be compared to the range obtained from the other PILPS schemes. Ignoring models which simulate less than 3000 mm of runoff (on the grounds that these models appear anomalous), the differences between mode RS and SLAM is 14.5% of the total range in runoff and 11.6% of the total evaporation range (ignoring the model which is well away from a line running through the scatter of the other models). It

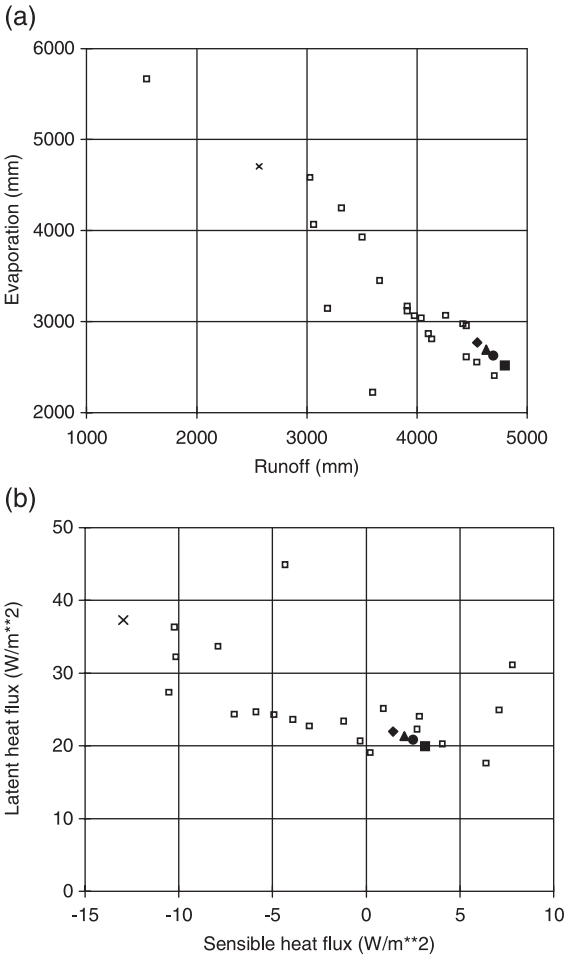

Fig. 8. Simulation of (a) evaporation (mm) and runoff (mm) and (b) latent and sensible heat fluxes (W m^{-2}) for each model in Phase 2(e) of PILPS. The five modes of CHASM are also shown. EB (×), RS (♦), RSI (▲), RSGI (●) and SLAM (■).

becomes subjective to omit increasing numbers of other models from the total range.

Fig. 8b shows the variation in the partitioning of available energy between sensible and latent heat fluxes. EB is again at the extreme of the range of PILPS models. The other four modes are within the range and vary by only 1.7 W m^{-2} in the case of the sensible heat flux and 2.0 W m^{-2} in the case of the latent heat flux. It is clear that a significant fraction of the overall scatter in the PILPS 2(e) results is unlikely to be explained by variations in the ways models simulate the SEB.

It is worth noting that the range of SEB complexity implemented in modes RS to SLAM is substantial and

probably larger than the range included within PILPS 2e. Despite this, variations in SEB complexity only explains 10–15% of the PILPS 2(e) scatter. If variations in the SEB complexity do not explain the differences found in the results, then the cause of the scatter shown in Figs. 7 and 8 must be related to the hydrology formulation (including the way the hydrology deals with snow processes). This is not a surprise (Gedney et al., 2000; Nijssen et al., 2003-this issue) but helps narrow the search for solutions.

6. Discussion and conclusions

This paper used the CHAmeleon Surface Model (CHASM) to explore the ability of the model to simulate the observed runoff for two sub-basins within the PILPS 2(e) domain. CHASM is designed to permit an exploration of the impact of SEB complexity on simulated fluxes since the SEB can vary from a simple Manabe (1969) type scheme to a more complex Deardorff (1978) type model. While the complexity of the SEB varies between modes, a common soil moisture and soil temperature model is used in all simulations.

CHASM is shown to simulate the observed runoff for two catchments with reasonable skill, but more important for this paper, this skill is shown to be largely insensitive to the complexity of the SEB parameterization, provided a spatially and temporally constant surface resistance is used. While in all bar, the least complex mode of CHASM (EB) works reasonably (within 5% of the observed runoff at Ovre Abiskojokk and within 15–20% at Ovre Lansjarv), there are weaknesses in the simulations, particularly at a seasonal time scale where the model tends to predict a too rapid snowmelt in early spring causing an over prediction of snow-related runoff. Later in spring, runoff is under predicted. However, these deficiencies are shown to be unrelated to the SEB complexity, and based on earlier analyses by, for example, Gedney et al. (2000) are most likely caused by weaknesses in the runoff or snowmelt formulations.

The results are also analysed spatially over the PILPS 2e domain. It is shown that the addition of a constant surface resistance into mode EB has a large impact on runoff and mode RS simulates much larger runoff over virtually the entire domain. This increase is the direct result of a reduction in the latent heat flux, which is reduced, following the imposition of a resistance, by more than 20 W m^{-2} over almost the entire domain. It is shown that the addition of an explicit parameterization of interception (RSI) and explicit bare soil evaporation has little effect on runoff or the latent heat flux, but the addition of a spatially and temporally variable surface resistance in the change between RSGI and SLAM does lead to an increase in the variability of runoff across the domain (Fig. 5e) and a small reduction ($\sim$ 5–10 W m^{-2}) in the latent heat flux.

Whether these changes are large or small is answered by comparing the differences in the results from the CHASM-modes to the results from the other PILPS Phase 2(e) models. It is shown that the differences between mode RS and SLAM are approximately 10–15% of the range in results from the other PILPS schemes. Given that the range of SEB complexity implemented in modes RS to SLAM is probably larger than that used in most other PILPS schemes, it suggests that SEB complexity does not explain the differences found in the results from PILPS Phase 2(e). If the differences are not due to the SEB complexity, then they are likely to be caused by differences in the hydrology formulation, including differences in how snowmelt is parameterized and distributed between infiltration and runoff. The significance of the snow and runoff processes in explaining the differences in model simulations for these experiments was discussed in detail by Nijssen et al. (2003-this issue). Our results, produced independently and with a very different methodology from Nijssen et al. (2003-this issue), produce similar conclusions.

In summary, our results point to the importance of the hydrological (including snow) components of land surface models. We identified few significant gains in adding complexity in the parameterization of the SEB beyond a constant surface resistance except in the pattern of runoff and evaporation across the domain. Residual weaknesses in CHASM's performance in simulating runoff are unlikely to be addressed through improving aspects of the SEB, rather our results point to the need to improve the hydrological parts of the model including snowmelt processes. We can only speculate on where the weaknesses are within the hydrological parts of the model, but based on Gedney et al.'s (2000) and Nijssen et al.'s (2003-this issue)

analyses, it is quite likely to be related to the runoff parameterization exacerbated in our simulations by a poor representation of snowmelt infiltration. We suggest that the recent focus on the hydrological component of land surface schemes and the reformulation of the problem in terms of catchments rather than grid squares (Koster et al., 2000), and the inclusion of runoff routing are likely to be fruitful in improving land surface models further.

Acknowledgements

YX thanks those attending the PILPS 2e workshop for both technical help and fruitful discussions. We all thank Laura Bowling and Dennis Lettenmaier for their considerable efforts in facilitating this phase of PILPS. This work was funded in part by the Australian Research Council.

References

Bonan, G.B., 1995. Land–atmosphere CO_2 exchange simulated by a land surface process model coupled to an atmospheric general circulation model. J. Geophys. Res. 100, 2817–2831.

Bowling, L.C., Lettenmaier, D.P., Nijssen, B., Graham, L.P., Clark, D.B., El Maayar, M., Essery, R., Goers, S., Habets, F., van den Hurk, B., Jin, J., Kahan, D., Lohmann, D., Mahanama, S., Mocko, D., Nasonova, O., Samuelsson, P., Shmakin, A.B., Takata, K., Verseghy, D., Viterbo, P., Xia, Y., Ma, X., Xue, Y., Yang, Z.-L., 2003. Simulation of high latitude hydrological processes in the Torne-Kalix basin: PILPS Phase 2(e) 1: Experiment description and summary intercomparisons. Glob. Planet. Change 38, 1–30.

Chen, T.H., Henderson-Sellers, A., Milly, P.C.D., Pitman, A.J., Beljaars, A.C.M., Polcher, J., Abramopoulos, F., Boone, A., Chang, S., Chen, F., Dai, Y., Desborough, C.E., Dickinson, R.E., Dumenil, L., Ek, M., Garratt, J.R., Gedney, N., Gusev, Y.M., Kim, J., Koster, R., Kowalczyk, E.A., Laval, K., Lean, J., Lettenmaier, D., Liang, X., Mahfouf, J.-F., Mengelkamp, H.-T., Mitchell, K., Nasonova, O.N., Noilhan, J., Robock, A., Rosenzweig, C., Schaake, J., Schlosser, C.A., Schulz, J.-P., Shmakin, A.B., Verseghy, D.L., Wetzel, P., Wood, E.F., Xue, Y., Yang, Z.-L., Zeng, Q., 1997. Cabauw experimental results from the project for intercomparison of land-surface parameterisation schemes. J. Climate 10, 1144–1215.

Cogley, J.G., Pitman, A.J., Henderson-Sellers, A., 1990. A model of land surface climatology for General Circulation Models, Trent Tech. Note, 90-1, Trent University, Canada.

Crossley, J.F., Polcher, J., Cox, P.M., Gedney, N., Planton, S., 2000. Uncertainties linked to land surface processes in climate change simulations. Clim. Dyn. 16, 949–961.

Deardorff, J.W., 1978. Efficient prediction of ground surface temperature and moisture with inclusion of a layer of vegetation. J. Geophys. Res. 83, 1889–1903.

Desborough, C.E., 1999. Surface energy balance complexity in GCM land surface models. Clim. Dyn. 15, 389–403.

Desborough, C.E., Pitman, A.J., 1998. The BASE land surface model. Glob. Planet. Change 19, 3–18.

Desborough, C.E., Pitman, A.J., McAvaney, B., 2001. Surface energy balance complexity in GCM land surface models. Part II: coupled simulations. Clim. Dyn. 17, 615–626.

Dickinson, R.E., Henderson-Sellers, A., Kennedy, P.J., 1993, Biosphere-Atmosphere Transfer Scheme (BATS) Version 1e as Coupled to the NCAR Community Climate Model. NCAR Technical Note TN- 387 + STR, August 1993. 72 pp.

Dirmeyer, P.A., Dolman, A.J., Sato, N., 1999. The pilot phase of the global soil wetness project. Bull. Am. Meteorol. Soc. 80, 851–878.

Ducharne, A., Koster, R.D., Suarez, M.J., Stieglitz, M., Kumar, P., 2000. A catchment-based approach to modeling land surface processes in a general circulation model 2. Parameter estimation and model demonstration. J. Geophys. Res. 105, 24823–24838.

Gedney, N., Cox, P.M., Douville, H., Polcher, J., Valdes, P.J., 2000. Characterising GCM land surface schemes to understand their responses to climate change. J. Climate 13, 3066–3079.

Henderson-Sellers, A., Pitman, A.J., Love, P.K., Irannejad, P., Chen, T., 1995. The project for intercomparison of land surface parameterisaton schemes PILPS Phases 2 and 3. Bull. Am. Meteorol. Soc. 76, 489–503.

Kojima, K., 1967. Densification of seasonal snow cover. Physics of Snow and Ice. Proc. Int. Conf. Low Temp. Sci., vol. 1 (2), pp. 929–952.

Koster, R.D., Suarez, M.J., 1992. Modelling the land surface boundary in climate models as a composite of independent vegetation stands. J. Geophys. Res. 97, 2697–2715.

Koster, R.D., Suarez, M.J., 1994. The components of a SVAT scheme and their effects on a GCM's hydrological cycle. Adv. Water Resour. 17, 61–78.

Koster, R.D., Milly, P.C., 1997. The interplay between transpiration and runoff formulations in land surface schemes used with atmospheric models. J. Climate 10, 1578–1591.

Koster, R.D., Suarez, M.J., Ducharne, A., Stieglitz, M., Kumar, P., 2000. A catchment-based approach to modeling land surface processes in a general circulation model 1. Model structure. J. Geophys. Res. 105, 24809–24822.

Manabe, S., 1969. Climate and the ocean circulation: I. The atmospheric circulation and the hydrology of the earth's surface. Mon. Weather Rev. 97, 739–805.

Nijssen, B., Bowling, L.C., Lettenmaier, D.P., Clark, D.B., El Maayar, M., Essery, R., Goers, S., Gusev, Y., Habets, F., van den Hurk, B., Jin, J., Kahan, D., Lohmann, D., Ma, X., Mahanama, S., Mocko, D., Nasonova, O., Niu, G.-Y., Samuelsson, P., Shmakin, A.B., Takata, K., Verseghy, D., Viterbo, P., Xia, Y., Xue, Y., Yang, Z.-L., 2003. Simulation of high latitude hydrological processes in the Torne-Kalix basin: PILPS Phase 2(e) 2: Comparison of model results with observations. Glob. Planet. Change 38, 31–53.

Noilhan, J., Planton, S., 1989. A simple parameterization of land surface processes for meteorological models. Mon. Weather Rev. 117, 536–549.

Pitman, A.J., McAvaney, B.J., The role of surface energy balance complexity in land surface models in controlling the sensitivity of surface and near-surface quantities to increasing carbon dioxide. Climate Dynamics. In press.

Pitman, A.J., Henderson-Sellers, A., Yang, Z.-L., Abramopoulos, F., Boone, A., Desborough, C.E., Dickinson, R.E., Gedney, N., Koster, R., Kowalczyk, E., Lettenmaier, D., Liang, X., Mahfouf, J.-F., Noilhan, J., Polcher, J., Qu, W., Robock, A., Rosenzweig, C., Schlosser, C., Shmakin, A.B., Smith, J., Suarez, M., Verseghy, D., Wetzel, P., Wood, E., Xue, Y., 1999. Key results and implications from Phase 1(c) of the project for intercomparison of land-surface parameterization schemes. Clim. Dyn. 15, 673–684.

Polcher, J., Laval, K., Dümenil, L., Lean, J., Rowntree, P.R., 1996. Comparing three land surface schemes used in GCMs. J. Hydrol. 180, 373–394.

Robock, A., Vinnikov, K.Ya., Schlosser, C.A., Speranskaya, N.A., Xue, Y., 1995. Use of midlatitude soil moisture and meteorological observations to validate soil moisture simulations with biosphere and bucket models. J. Climate 8, 15–35.

Sato, N., Sellers, P.J., Randall, D.A., Schneider, E.K., Shukla, J., Kinter III, J.L., Hou, Y.-T., Albertazzi, E., 1989. Effects of implementing the simple biosphere model in a general circulation model. J. Atmos. Sci. 46, 2757–2782.

Schlosser, C.A., Slater, A.G., Robock, A., Pitman, A.J., Vinnikov, K.Ya., Henderson-Sellers, A., Speranskaya, N.A., Mitchell, K., Boone, A., Braden, H., Chen, F., Cox, P., de Rosney, P., Desborough, C.E., Dickinson, R.E., Dai, Y.J., Duan, Q., Entin, J., Etchevers, P., Gedney, N., Gusev, Y.M., Habets, F., Kim, J., Koren, V., Kowalczyk, E., Nasonova, O., Noilhan, J., Shaake, J., Shmakin, A., Smirnova, T., Verseghy, D., Wetzel, P., Xue, Y., Yang, Z.L., 2000. Simulations of a Boreal grassland hydrology at Valdai, Russia: PILPS phase 2(d). Mon. Weather Rev. 128, 301–321.

Sellers, P.J., Mintz, Y., Sud, Y.C., Dalcher, A., 1986. A simple biosphere model (SiB) for use with general circulation models. J. Atmos. Sci. 43, 505–530.

Sellers, P.J., Randall, D.A., Collatz, C.J., Berry, J.A., Field, C.B., Dazlich, D.A., Zhang, C., Collelo, G., Bounoua, L., 1996. A revised land-surface parameterization (SiB2) for atmospheric GCMs. Part 1: model formulation. J. Climate 9, 676–705.

Sellers, P.J., Dickinson, R.E., Randall, D.A., Betts, A.K., Hall, F.G., Berry, J.A., Collatz, G.J., Denning, A.S., Mooney, H.A., Nobre, C.A., Sato, N., Field, C.B., Henderson-Sellers, A., 1997. Modelling the exchanges of energy, water and carbon between continents and the atmosphere. Science 275, 502–509.

Slater, A.G., Schlosser, C.A., Desborough, C.E., Pitman, A.J., Henderson-Sellers, A., Robock, A., Vinnikov, K.Ya., Mitchell, K., Boone, A., Braden, H., Chen, F., Cox, P., de Rosnay, P., Dickinson, R.E., Dai, Y.-J., Duan, Q., Entin, J., Etchevers, P., Gedney, N., Gusev, Y.M., Habets, F., Kim, J., Koren, V., Kowalczyk, E., Nasonova, O.N., Noilhan, J., Schaake, J., Shmakin, A.B., Smirnova, T.G., Verseghy, D., Wetzel, P., Xue, Y., Yang, Z.-L., Zeng, Q., 2001. The representation of snow in land-surface schemes: results from PILPS 2(d). J. Hydrometeorol. 2, 7–25.

Verseghy, D.L., McFarlane, N.A., Lazare, M., 1993. CLASS-A Canadian land surface scheme for GCMs. II: vegetation model and coupled runs. Int. J. Climatol. 13, 347–370.

Wood, E.F., Lettenmaier, D.P., Zartarian, V.G., 1992. A land-surface hydrology parameterization with subgrid variability for general circulation models. J. Geophys. Res. 97 (D3), 2717–2728.